NASA Contractor Report 195051

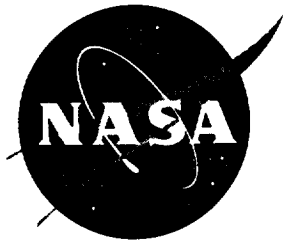

FAN NOISE PREDICTION ASSESSMENT

Paul H. Bent
McDonnell Douglas Aerospace, Long Beach, California

Contract NAS1-20103

May 1995

National Aeronautics and
Space Administration
Langley Research Center
Hampton, Virginia 23681-0001

ACKNOWLEDGMENT

The author would like to express his appreciation to the following people: Dr. A. Schmilovich and Mr. D. Halsey for their assistance in the compressible potential flow calculations; Mr. D. Topol of Pratt and Whitney for his cooperation and helpfulness with questions regarding the ARC code; and Mr. D. Huff of NASA Lewis Research Center for his sincere interest in helping with problems and questions. The author would also like to acknowledge Dr. J. Posey who was the NASA Technical monitor for this task.

1. INTRODUCTION

This report is an evaluation of two techniques for predicting the fan noise radiation from engine nacelles. The first is a relatively computational intensive finite element technique. The code is named ARC (an abbreviated form of ***A***coustic ***R***adiation ***C***ode) and was developed by Eversman.[1] This is actually a suite of software that first generates a grid around the nacelle, then solves for the potential flowfield, and finally solves the acoustic radiation problem. Only axisymmetric configurations can currently be analyzed with this program. The code requires a detailed description of the nacelle and centerbody geometry. It also requires that the modal amplitude and phase at a particular station in the duct be known. ARC can solve for the farfield radiation for any number of radial modes but only one circumferential mode number at a time.

The second approach is an analytical technique requiring minimal computational effort. This is termed the cutoff ratio technique and was developed by Rice.[2] Details of the duct geometry, such as the hub-to-tip ratio and Mach number of the flow in the duct, and modal content of the duct noise are required for proper prediction. Unlike the ARC program, however, modal phase information is not used. The radiated noise of each mode is calculated individually. The directivity patterns of all the modes are then summed to yield the total radiated noise. A closed form expression for the sound pressure directivity was derived by Rice and Sawdy[3] for the case of no external flow. Corrections to the directivity levels and mean square pressure magnitude were added to this formulation to account for the presence of external flow. A disadvantage of this technique is that without some form of calibration, the radiated noise sound pressure levels cannot be calculated. Comparisons of the radiated noise levels generated by different modes are, therefore, usually presented in terms of relative level.

In sections 2 and 3 of this report, details of the ARC and cutoff ratio techniques are described in greater detail. For each approach there is a discussion and critique of the operation of each of the programs. Section 4 presents a study of the influence of parameters such as duct Mach number on the directivity and level of the radiated sound. Sections 5 and 6 show the results of predictions of the far-field noise for various nacelle/duct configurations. Included are data obtained in an experimental investigation of the radiated noise of the Pratt and Whitney Advanced Ducted Propulsor (ADP) model tested in the 9x15 ft anechoic wind tunnel at NASA Lewis.[4] Other configurations include a bellmouth inlet and a more realistic 'flight' inlet modeled on a JT15 nacelle.[5] Both these inlets were tested in the NASA Langley spinning mode synthesizer facility.

The importance of providing the correct mode phase to the input of the ARC code is assessed in section 7. Since the flowfield solution is provided by the ARC program, the accuracy of the compressible flow correction used in the ARC code is assessed by comparison to solutions obtained from a true compressible potential flow solver for a range of Mach numbers in section 8. Finally conclusions and recommendations for the operation and application of these programs are given in section 9.

2. ARC FINITE ELEMENT TECHNIQUE

The Acoustic Radiation Code (ARC) is a finite element noise radiation code developed by Eversman *et al.*[1] to solve the problem of noise radiation from axisymmetric ducts. The code was adapted from the original IBM mainframe platform to run on Silicon Graphics™ and SUN™ workstations by Meyer.[6] Further minor modifications to the codes were made by the author for operation on a Hewlett Packard™ Apollo™ 735 workstation.

The ARC code is composed of five programs. The first two programs generate the finite element mesh around the nacelle. The next two solve the potential flowfield both inside and outside the nacelle. The final program solves the acoustic field which is posed as an harmonic problem. The flowfield and acoustic field formulations are cast in terms of potential. To simplify the formulation, the flowfield calculation is made for incompressible flow (i.e. the non-linear compressible form of the equations are reduced to the linear Laplace equation) and the results corrected to account for compressibility. To provide a non-reflecting boundary, 'wave envelope' layers are place at the edge of the domain (except on the axis of symmetry and a 'baffle' which is a boundary considered sufficiently far downstream on the nacelle inlet so as not to cause reflection problems in the acoustic solution).

ARC solves for the directivity of one circumferential mode order at a time. Any number of (cut-on) radial modes associated with that circumferential mode order are solved simultaneously. A reason for this restriction is that the input to the acoustic radiation component is in the form of real and imaginary modal amplitude. If, for example, there are several circumferential mode orders excited at the blade passage frequency, the rotational speed of each of these modes must be different. Therefore, at any one time, the relative phase between the circumferential modes will be different than for any other time. As is demonstrated in a later section, the relative phase between the modes plays an important part in determining the overall directivity pattern.

Appendix A contains a discussion of the various components that make up ARC. Included in this appendix are details of the code operation and idiosyncrasies involved in using ARC.

3. CUTOFF RATIO TECHNIQUE

The cutoff ratio technique was developed by Rice.[2] The theory is based on the observation that the principal far-field directivity angle is equivalent to the angle between the duct axis and the propagating acoustic spinning mode in the duct. The cutoff ratio, ξ, is the ratio between the frequency of the spinning mode and the cutoff frequency of that mode, defined thus

$$\xi = \frac{kr_0}{\alpha\sqrt{1 - M_D^2}} \tag{1}$$

where k is the wave number (ω / c), r_0 is the duct radius, α is the hardwall duct eigenvalue for the mode, and M_D is the duct Mach number. The value of α depends on the circumferential and radial mode order and the hub to tip ratio and is defined as the value at which the derivative of the Bessel function of the first kind is zero. If ξ is greater than unity, the mode will propagate. If less than unity, the mode decays exponentially. The radical in the denominator of equation (1) accounts for the influence of duct flow on the cutoff ratio.

In a development of the original work by Rice and Sawdy,[3] an expression was derived that gave a closed form algebraic solution for the radiated noise directivity for the case of flow in the duct but zero external flow. Since this expression is lengthy it is not repeated here. Modifications to account for the effect of external flow on the directivity angle and mean square sound pressure were derived in another work by Rice and Heidmann.[8] These are

$$\cos\psi_p = \frac{(M_\infty + \cos\varphi)}{\sqrt{1 + M_\infty^2 + 2M_\infty \cos\varphi}} \tag{2}$$

$$\frac{p_\infty^2}{p_0^2} \approx \frac{(1 + M_\infty^2 + 2M_\infty \cos\varphi)^{3/2}}{(1 + M_\infty \cos\varphi)} \tag{3}$$

where ψ_p is the principal angle of the main directivity lobe, M_∞ is the free field Mach number, φ is the wave front propagation angle relative to the duct axis, p_∞ is the far-field pressure after the external flow correction has been made, and p_0 is the far-field pressure under static conditions.

These expressions have been combined in a computer program that, given the duct characteristics of hub to tip ratio and Mach number, first calculates the duct eigenvalue, α, and then the cutoff ratio for the desired mode. If the cutoff ratio is greater than 1.0, the mode is cut-on and the far-field directivity is predicted. In comparisons of the relative

noise levels generated by a different radial modes, the amplitude of the farfield noise is multiplied by the relative strength of the mode in the duct (if known). Since the technique (as applied here) is set up for equal power per mode predictions, the multiplication of the farfield amplitudes by the duct amplitude is appropriate.

To determine the total far-field noise radiation from multiple duct modes, the mean square pressure of each of the individual modes predicted by the cutoff ratio technique are summed within particular directivity angle bins. In the case of data presented here, the directivity angle bin width is 2°. This is similar to the approach adopted by Topol[4] for predicting the total radiated noise from multiple circumferential modes in the finite element ARC technique.

Verification of the program was made for the case of no external flow against test cases described in Rice and Sawdy.[3] The test cases from this reference and the equivalent calculations from the current program are shown in Figure 1. The cutoff ratio approach has the advantage over the finite element ARC approach in that the user has to supply much less information about the geometry of the nacelle or duct. The principal disadvantage is that without a calibration procedure to account for the reflection properties of different duct inlet geometries, only relative levels of sound between modes can be determined.

4. PARAMETRIC STUDY OF ARC AND CUTOFF RATIO PREDICTIONS

To determine how various parameters affect the predictions of radiated noise from the ARC code and the cutoff ratio approach, the two techniques were used to predict the farfield noise radiated from a duct. While keeping all other parameters constant, the circumferential mode order, radial mode order, and inlet duct Mach number were varied systematically and the predictions compared.

In addition to the effect of the parameters listed above, the effect of inlet geometry is also investigated. The cutoff ratio technique is theoretically based on a flanged duct configuration. Nacelle inlet configurations are typically not of this geometry. Therefore, to illustrate what limitations the cutoff ratio might encounter when attempting to predict the radiated noise from a nacelle, the finite element ARC predictions are made for a bellmouth inlet configuration shown in Figure 2. The geometry of the inlet was taken from an investigation by Silcox.[5]

For all the comparisons described below, the normalized frequency, η ($=kr_o$), was held constant at 10.0. The free field Mach number was kept at zero and the hub-to-tip ratio, σ, also remained at zero. For the computations, the input mode amplitude was set to unity in all cases. The reader should note that only the relative levels of the modes are shown. The quantity shown is the mean square pressure it is plotted on a linear scale. Furthermore, the relative levels between the cutoff ratio predictions and the ARC predictions has no direct significance.

Circumferential Mode Order

Figures 3(a) and 3(b) show the farfield predicted noise when the circumferential mode order is varied between 2 and 8 for the cutoff ratio and ARC techniques, respectively. Only the zeroth order radial mode is calculated. The peak directivity angles for mode (2,0) and (4,0) compare very well being approximately 18° and 32°, respectively. Mode (8,0), however, does not compare well. In the cutoff ratio technique, the farfield angle is calculated to peak at approximately 73° whereas the ARC code places the peak directivity in the order of 48°. Within each figure, however, the relative level of the modes is relatively close. Each technique shows a decreasing magnitude of radiated noise with increasing mode order with approximately the correct proportion.

Radial Mode Order

Figures 4(a) and 4(b) show the farfield directivity for different radial mode orders of the same circumferential mode. In this example, the modes orders are (2,0), (2,1), and (2,2). Distinctly different trends are observed in these figures. As in the previous set of figures, there is qualitatively good agreement for the (2,0) mode. For the (2,1), however, the cutoff ratio approach shows a major lobe only at approximately 42°, but the ARC approach has a double lobed directivity with lobes centered on 38° and 15°. An even more drastic difference is observed in the directivity of the (2,2) mode. With the cutoff

ratio technique, the main lobe, although very flat, is centered on approximately 80°. The ARC code, however, shows a triple lobe pattern with the highest magnitude seen at 14°.

One explanation for this behavior may be the excitation of other duct modes due to the sound propagation in the duct, the duct geometry, and the effects of duct termination reflection. None of these effects are captured with the cutoff ratio approach. In Figure 4 it can be seen that the number of distinct lobes (as opposed to side lobes) observed in the directivity pattern generated by ARC is the same as the radial mode order plus 1. That is, the mode (2,1) actually produces two lobes. The directivity angles of these lobes correspond to the angle for the mode in question (the highest of the angles) and the also the approximate angles of the lower order radial modes. So the mode (2,1) produces lobes that correspond in angle to modes (2,1) and (2,0). The higher radiation efficiency of the lower order radial modes may sometimes lead to the excited lower order mode lobe being dominant (as is the case of mode (2,2) in Figure 4(b) where the lobe corresponding to mode (2,0) is the highest in magnitude).

Inlet Duct Mach Number

The influence of the duct flow Mach number is shown in Figures 5(a) and 5(b) for the cutoff ratio and ARC techniques, respectively. In these figures the duct Mach number is varied between 0.0 and 0.6 for the (2,1) duct mode. The cutoff ratio technique shows a steady decrease in directivity angle and increase in amplitude with increasing duct Mach number. The effect of increasing the duct Mach number is to increase the cutoff ratio of the mode (see equation 1). The trends in the directivity pattern with amplitude, directivity angle and cutoff ratio predictions are also seen in the ARC results. For the case of the ARC predictions, increasing the duct Mach number also has the effect of redistributing the principal radiation lobe toward lower angles. Unlike the cutoff ratio technique, however, there is no accompanying increase in amplitude. In fact the amplitude decreases with increasing duct Mach number.

Review

This parametric study has shown that the cutoff ratio technique and the ARC approach have some common trends in the prediction of farfield noise. Increasing mode order generally increases directivity angle and reduces amplitude in both techniques, for example. There are some important differences, however. Whereas the cutoff ratio approach shows trends in amplitude and directivity that are solely dependent on the cutoff ratio, the ARC predictions shows considerably more complicated trends. The generation of multiple lobe directivity pattern with higher order radial modes being just one example. In addition, the predicted directivity lobe width is much greater with the ARC technique than with the cutoff ratio approach. In the following sections, the predictions of both the cutoff ratio and ARC techniques are compared to measured data to determine which of the two best predict the character of the radiated noise.

5. COMPARISON OF MEASURED NOISE DIRECTIVITY AND PREDICTIONS FOR SIMPLE GEOMETRIES

A literature survey was conducted to locate sources of duct radiated noise data where information regarding the modal content of the noise in the duct is also available. One source of experimental data is given by Silcox.[5] This report describes a series of experiments on two different inlet geometries that were tested in the NASA Langley Spinning Mode Synthesizer/Flow Duct Facility. With this apparatus, duct modes are generated artificially using an array of loud speakers. The facility also allows flow in the duct to be generated so that this effect can be investigated. The far-field noise is measured at a constant radial distance from the inlet using a boom mounted microphone. The two inlet configurations tested were a bell mouth inlet and a "flight inlet" representative of an inlet fitted to a JT15 engine in a different investigation. Neither of these geometries have centerbodies (i.e. σ=0.0). These inlets are shown in Figure 6 along with the Mach number distribution in the duct for the case M_D=0.4

Flight Inlet

Figure 7 shows the measured radiated noise directivity of duct mode $(2,0)^5$ for the flight inlet with normalized frequency, $kr_0 = 3.72$, with ($M_D = 0.4$) and without flow. Figures 8 and 9 show the predictions obtained from the ARC and cutoff ratio codes respectively. As with the experimental data, the levels of the radiated noise have been normalized by the highest level obtained with either the flow on or off.

The ARC prediction shown in Figure 8 matches the directivity angle of the peak level of noise very closely. The general shape of the directivity is also close to the measured shape but the prediction trails off more rapidly at both high and low directivity angles. This may be due to extraneous modes being generated by the mode synthesizer in the experiments and 'filling out' the radiated noise directivity. One of the most significant observations is that, like the measured data, there is no great change in the directivity pattern. In the measured data, there is a 2 - 4 dB difference in the level between the cases with and without flow. In the ARC predictions there is 1 - 2 dB change in the level of the radiated noise. Overall, the agreement between the measured data and the ARC prediction is considered to be good.

Figure 9 shows the comparable predictions of the flight inlet directivity made using the cutoff ratio technique. For the no flow case, the peak directivity angles are slightly over predicted. The shape of the lobes, though, are substantially different being much narrower than the measured data. For the prediction of the duct with flow, the comparison with experimental data worsens. Instead of remaining similar in shape to the no flow case, the lobe becomes higher, peaks at a much smaller angle, and becomes narrower. Generally, the behavior of the cutoff ratio prediction for the flight inlet does not compare well with the measured data.

Bellmouth Inlet

Figure 10 shows the measured directivity of a bellmouth inlet when radiating a dominant (2,1) mode at a normalized frequency of $\eta = 8.18$ (duct mode (2,0) is also measured in the duct and included in the calculations but at a lower magnitude). Two cases are shown: one for a duct Mach number of 0.0 and the other for 0.2. Figure 11 shows the ARC prediction for this configuration. As with the flight inlet, the drop off of the lobes is much greater than with the measured data. The relative level of the lobe at higher directivity angle is grossly under predicted (or, since the directivity lobes are plotted as relative magnitudes, it may be said that the level of the lower angled lobe is over predicted). The peak angle of these lobes match the measured data very well. Like the flight inlet, there is a much greater difference in level between the cases with and without flow in the measured data than the ARC predictions.

There is reasonable agreement between the measured data and the cutoff ratio predictions (see Figure 12). As before, the directivity angles are slightly over predicted for the no flow case and slightly under predicted for the case with flow in the duct. Although the higher angle lobes have a higher magnitude than the lower angle (opposite to the trend in the data), they are closer to predicting the true relative level of the data than the ARC predictions. Because two modes are being added in this case (the (2,0) and the (2,1)), there are smaller valleys between the peaks which looks more like the experimental data than the ARC prediction.

Review

Overall, the ARC prediction scheme predicts the directivity pattern of these relatively simple geometries very well, particularly in terms of directivity angle. The cutoff ratio also predicts the peak directivity angles reasonably well but often fails to capture the fullness of the lobes of the directivity pattern. The potential refraction effects of the inlet geometry that the ARC code can capture but the cutoff ratio theory cannot (since it is based on a flanged duct geometry) may account for this discrepancy. It is also interesting to observe that the ARC solution showed no change in directivity with increasing duct flow in a static test which agreed well with the measured data but is contrary to the predictions of the cutoff ratio technique.

6. COMPARISON OF THE MEASURED NOISE DIRECTIVITY AND PREDICTIONS FOR THE ADP CONFIGURATION

The Acoustic Radiation Code (ARC) and the Cutoff ratio code have been applied to calculate the far-field noise of the Pratt and Whitney 17.25 inch diameter Advanced Ducted Propulsor (ADP) model that was tested in the 9 x 15 ft anechoic wind tunnel at the NASA Lewis Research Center. The ADP has an advanced design fan with 16 blades. A sketch of the ADP nacelle is shown in Figure 13. The wind tunnel was operated so that the free stream Mach number was 0.2 to simulate landing and takeoff conditions. The wind tunnel can be considered anechoic for all frequencies of interest. An excellent report showing the comparison of the predictions of the ARC code and the measured data has been made by Topol.[4] It is not intended that this section shall be a reiteration of this work. Instead, the object of these comparisons shall be the relative accuracy of the ARC and cutoff ratio techniques.

Several geometries were investigated in these experiments including a long and medium inlet configuration. Fan speeds ranging from 9 600 to 11 400 RPM (the maximum tip speed for the fan is 275.2 m/s (Mach 0.81) at 12 000 RPM), and different number of exit guide vanes (22 and 40) to generate different number of cut-on modes were also examined. The ADP test facility was also fitted with a rotating microphone array mounted upstream of the fan row to measure the spinning acoustic modes in the duct. Both amplitude and phase of the spinning circumferential and radial modes are measured with this facility. The rotating microphone array measured the properties of the acoustic modes at only one axial station in the duct, however. It was, therefore, impossible to decompose the measured data into forward propagating and reflected waves. In data published from these experiments (Heidelberg[9]) it was assumed that the data were mostly composed of forward propagating waves.

The ADP was designed to generate only the -6 circumferential mode order in the 22 vane configuration. Irregularities in the fan casing tip treatment, however, caused additional modes to be generated. To make direct comparison to the measured data it was, therefore, necessary to rely entirely on the measured acoustic modal information rather than predictions of the mode amplitude from such programs as V072 (developed at Pratt and Whitney under NASA funding)[4] since the extraneous modes would not have been predicted. Topol[4] has performed an extensive comparison of the use of mode amplitude predictions and measured data on the prediction of far-field noise.

In the following sections, the predictions of the far-field noise derived by both the finite element and cutoff ratio techniques are compared to measured experimental data for various configurations and conditions. Since the cutoff ratio technique yields only relative levels of sound, it was necessary to fix the level of the directivity pattern so that a meaningful comparison could be made. This was accomplished by forcing the level of the cutoff ratio prediction to match the level of the ARC prediction at the peak amplitude.

BPF, Medium Inlet, 22 Vanes, 9 600 RPM

Figures 14(a) and 14(b) show the finite element and cutoff ratio predictions of the radiated far-field noise, respectively. This directivity pattern is made up of ±4, -6 and ±8 modes. For the cutoff ratio, it is important to specify the conditions at the end of the duct. Therefore, in these figures, the duct Mach number was set equal to the free stream value of 0.2 and the hub-to-tip ratio, σ, was set equal to zero. The mode amplitudes were specified to be the same as those specified as the input to the ARC computation.

An obvious difference between the two predictions is the relative smoothness of the curve representing the ARC prediction. The explanation for this is that the cutoff ratio figure is the sum of a series of curves for each of the modes present. Each of these modal directivities tend to be much narrower than the comparative directivity pattern generated with the ARC technique (as was observed in the preceding section). There will, therefore, tend to be fewer 'gaps' in between the individual mode directivities in the ARC approach, leading to a much smoother overall directivity.

Although discussion of the level prediction is meaningless since the level of the cutoff ratio prediction is artificially set, the shape of the directivity pattern is worthy of remark. The overall shape of the two curves is somewhat similar except in the region less than 50°. For the ARC prediction, the level remains high and drops off rapidly between 30° and 0°. There is insufficient measured data at shallow directivity angles to determine which of the two solutions is better.

2BPF, Medium Inlet, 22 Vanes, 9 600 RPM

Figures 15(a) and 15(b) show similar data to above but for the second harmonic of the BPF. Again the input conditions for the cutoff technique were assumed at the nacelle inlet. In this example there is quite good agreement between the measured data and the cutoff ratio prediction. Allowing for the fact that the level of the cutoff ratio prediction is set to match that of the ARC prediction at the highest level, there are a remarkable number of points where the curve passes through the measured data. It may be argued that the ARC prediction would also fit through more points should the level of the curve be reduced by approximately 7dB.

Review

Both the ARC and cutoff ratio predictions show reasonably good agreement with the measured data from the experiments on the ADP configuration. The ARC has the distinct advantage of being capable of predicting the level of the radiated noise as well as the directivity. If all that is desired is an estimation of the directivity characteristics, this comparison indicates that the cutoff ratio would yield satisfactory results.

7. EFFECT OF RELATIVE MODE PHASE ON THE ARC FAR-FIELD NOISE PREDICTIONS

One important consideration when using the ARC is the relative phase between the individual radial modes in a single calculation. The ARC code converts the given modal amplitude and phase for each of the radial modes into the equivalent pressure on the fan face. The pressure distribution of all the modes are then summed to give the pressure boundary condition on the fan face. Obviously the specified relative phase of the duct modes will affect this pressure distribution.

To estimate the possible magnitude of an error in the given phase of the radial modes, the measured relative phase of the (4,0) mode was shifted while keeping the phase of the (4,1) mode constant in the input data for the ADP configuration[4] (for the case of the ADP operating at 9600 RPM, medium inlet, 22 vanes, blade passage frequency). The original phase of the (4,0) mode is 67.17° and the adjusted phase is 270°. The phase of the (4,1) mode is -14.37° in both computations. The resulting radiated noise pressure contour plot of the original phase and the modified phase can be seen in Figures 16 and 17, respectively.

The difference in the pressure on the fan face is easily observed. In the correct phase relationship, there is an obvious node on the fan face. In the radiated sound, the effects of both the (4,0) and the (4,1) modes are clearly seen. Mode (4,0) produces the lobe at approximately 35° and mode (4,1) produces the lobe at approximately 70°. There is a clearly defined null between these two lobes.

In Figure 17, the pressure distribution on the fan face is looks similar to one that would be produced by a single mode of zero radial mode order. The directivity pattern of this combination of radial modes also looks like it was generated by a single duct mode. There is no longer an obvious null between two lobes as was seen with the original modal distribution.

Review

One implication of this sort of analysis is that it shows dramatically that adjusting the relative phase between modes can potentially be used to control the noise radiated by turbofan engines. It may be possible to design an engine that generates duct modes with specific relative phases. In addition to controlling the far-field radiation directivity in this way, it may also be possible to tailor duct mode generation so that the most attenuation possible of these modes could be derived from duct liners which in turn are designed for the greatest attenuation of particular modes.

8. ACCURACY ASSESSMENT OF THE POTENTIAL FLOW CALCULATION OF THE ARC CODE

One stage of the ARC calculation is to compute the potential flowfield around the nacelle. Partially to simplify this computation, the formulation is cast as an incompressible flow field and the problem reduces to that of solving the Laplace equation. Later in the computation a compressibility correction is applied to the Mach number calculation to provide more realistic values. In the discussion of the cutoff ratio technique in section 3 (equations (1) through (3)), it was shown that the Mach number of the flow in the duct can play a role in the propagation characteristics of acoustic duct modes. The accuracy of the compressibility correction can, therefore, affect the accuracy of the acoustic solution. In this section, a comparison is made between the flow field computed with the ARC code and that of a true compressible potential flow solver (abbreviated to CPFS in the discussion below) developed at McDonnell Douglas on a refined grid.

The Pratt and Whitney ADP configuration was chosen for the comparison. The particular configuration used was the medium inlet / short spinner configuration as defined for use with the predictions of fan noise from the V072 noise generation prediction program. This configuration has the interior of the nacelle defined up to the fan exit guide vane location.[4] A definition of the nacelle interior to a point where the cross sectional area is constant is a requirement of the compressible potential flow solver used here. It should be noted that the waviness of the walls on the interior of the nacelle in the figures discussed below is how the geometry is defined and not an artifact of poor grid generation.

The flow is solved over a range of Mach numbers defined at the fan face (M_D= 0.2, 0.5, and 0.7) for a single free stream Mach number (M_∞= 0.2). To give both a qualitative and qualitative comparison of the different methods, the solutions obtained from ARC and the compressible potential flow solver are plotted both on a contour plot and in a plot of the radial Mach number distribution in the duct at axial station X=0. This station is approximately half-way between the nacelle inlet and the fan face and represents a good location for comparison. The fan face itself cannot be used for comparison as the Mach number is defined there as a boundary condition.

Figures 18 and 19 show the Mach number Magnitude plots of the ARC and CPFS solutions, respectively, for the case of M_D= 0.2. Qualitatively, the contour plots agree reasonably well. The stagnation points are in the same location and have approximately the same character. The rougher appearance of the ARC solution (especially in the vicinity of the stagnation point on the highlight) is due to the nature of the computational grid in those locations. The Mach number distribution at X=0 show in the inserted window in each figure shows approximately the same profile but the CPFS values are approximately 4% higher in magnitude.

For the case of M_D= 0.5, shown in Figures 20 and 21 for the ARC and CPFS respectively, the comparison is not as close as for M_D= 0.2. As expected, the stagnation point moves along the upper surface of the nacelle in both solutions. The contours in the interior of the nacelle show quite different properties, however. The magnitude of the Mach number is considerably higher in the ARC solution (Figure 21) than in the CPFS solution (Figure 22). The plot of the Mach number at X=0 clearly demonstrates this observation. Although the shape of the Mach number profile is similar, the magnitude of the CPFS is approximately 10% lower than the ARC solution.

The trend toward over prediction of the duct Mach number by the ARC solution is also seen for the case of M_D= 0.7 shown in Figures 22 and 23 for the ARC and CPFS, respectively. Again the stagnation point on the nacelle moves along the upper surface in both solutions. There are significant differences in the two solutions, however, which are most clearly seen in the Mach number distribution at X=0 plot. The CPFS solution has a much less exaggerated difference between the inner and outer duct walls. At the inner wall, the difference between the two solutions is approximately 10.5% and at the outer wall the difference is 6.5%. In each case the ARC solution is larger.

Review

The discrepancy between the compressibility-corrected ARC code solutions and the more accurate true compressible potential flow calculations may indicate a possible inaccuracy in the noise predictions. If the mode is close to cut-on, errors on the order of 10% in the Mach number calculation could influence the propagation characteristics in the duct and hence the far field radiated noise directivity.

9. CONCLUSIONS AND RECOMMENDATIONS

In this report the finite element Acoustic Radiation Code (ARC) and the analytical cutoff ratio technique have been evaluated for their capability to predict noise directivity from a duct. The influence of circumferential and radial mode order and duct Mach number on the directivity angle and relative magnitude of the directivity lobes was assessed. Each technique was also evaluated for its capability to predict measured radiated noise from a variety of duct/nacelle geometries.

The trends in the directivity predictions of both approaches with changes in circumferential and radial mode order are quite similar for higher cutoff ratios. For cutoff ratios closer to one, the similarity between the two techniques breaks down and generally poor agreement is seen. In addition the effects of duct Mach number appear to be poorly captured by the cutoff ratio technique when compared to ARC. In some circumstances, it appears that removing this parameter from the cutoff ratio technique may yield better agreement with measured data. Another characteristic that is seen for all cutoff ratios is that the directivity lobes predicted by the cutoff ratio technique tend to be much narrower than those of the ARC code predictions. Better agreement may be obtained by approximately doubling the width of the lobes.

The narrowness of the lobes predicted by the cutoff ratio tend to limit the agreement with measured data. The ARC code, conversely, tends to capture the shape of the radiated noise directivity well. In the case of multiple mode generation, care must be taken to properly define the mode phasal relationships or the resulting directivity pattern will likely be in error. The cutoff ratio does not have this problem, as the directivity of the modes is computed independently. Any potential interaction of the modes is lost in this approach, however. Another shortcoming of the cutoff ratio technique is the inability to capture the possible excitation of extra duct modes due to the propagation and reflection characteristics of the duct geometry.

In general, the ARC provided accurate predictions of both the directivity shape and the level of the measured data. The cutoff ratio code provided a reasonable approximation to the actual directivity pattern but, without a calibration procedure, cannot yield the level of the radiated noise. In fact neither approach can yield true farfield levels without knowledge of the actual duct mode strength. The cutoff ratio approach, however, has the advantage that is very simple to program and use. ARC on the other hand requires a powerful computer with a great deal of memory (over 100 Mb of temporary storage files are created during execution). Therefore, for quick estimates of the noise directivity, the cutoff ratio technique is recommended. If accuracy in terms of level and directivity lobe shape is required and the modal characteristics in the duct are known, however, the ARC code ought to be used. The most valuable application of the cutoff ratio technique (that was not discussed here) is as a design tool for broadband liners.

REFERENCES

1 Parrett, A.V., "Wave Envelope and Finite Element Approximations for Turbofan Noise Radiation in Flight," AIAA Journal, Vol. 24, No. 5, 1986, pp. 753-760.

2 Rice, E.J., "Multimodal Far-Field Acoustic Radiation Pattern Using Mode Cutoff Ratio," AIAA Journal, Vol. 16, No. 9, 1978, pp. 906-911.

3 Rice, E.J., and Sawdy, D.T., Theoretical Approach to Sound Propagation and Radiation for Duct with Suppressors," NASA TM 82612, 1982.

4 Topol, D.A. and Philbrick, D.A., "Fan Nose Prediction System Development: Wake Model Improvements and Code Evaluations," Prepared under contract NAS3-25952 Task 10, 1993.

5 Silcox, R.J., "Geometry and Static Flow Effects on Acoustic Radiation from Ducts," AIAA Journal, Vol 22 No.8, August 1984.

6 Meyer, H. D., "Fan Noise Prediction System Development: Source/Radiation Field Coupling and Workstation Conversion for the Acoustic Radiation Code," Prepared under contract NAS3-25952, 1994.

7 Danda-Roy, I., Eversman, W. and Meyer, H.D., "Improved Finite Element Modeling of the Turbofan Engine Inlet Radiation Problem," Prepared under contract NAS3-25952 Task 10, 1993.

8 Rice, E.J., and Heidmann, M.F., "Modal propagation Angles in a Cylindrical Duct with Flow and their Relation to Sound Radiation," AIAA Paper 79-0183, 1979.

9 Heidelberg, L.J. and Hall, D.G., "Acoustic Mode Measurements in the Inlet of a Model Turbofan Using a Continuously Rotating Rake," NASA TM 105989, 1993.

10 Lieblein, S., and Stockman, N.O., "Compressibility Corrections for Internal Flow Solutions," Journal of Aircraft, Vol. 9, No. 4, pp. 312-313, 1972.

APPENDIX A

In this discussion of the components making up the ARC code, the name of the programs are given in capital letters to make them easily distinguishable. The file name extension ('.f' on UNIX™ systems) indicating they are FORTRAN files is implied. The name of the files correspond to generic names for the programs. Different versions of the programs have been given different suffixes depending on their content. Releases from the development work from Hamilton Standard, for example, have 'h' suffixes to indicate their source. These have been dropped for the purposes of this discussion.

This section contains a discussion of the purpose of the various components that make up the ARC code. Included in this section are comments regarding any difficulties or complications encountered in their use.

ARC Component Description

Mesh Generation

The first two components of the ARC code are for mesh generation: these are PRATPRE and PRATMESH. The input to PRATPRE is the nacelle and centerbody geometrical information and instructions for the relative placement of the surface element nodes (specified in terms of percentages of the (horizontal) length of the component). It was found that the proper placement of the finite elements was often a trial and error procedure. Typically it was not until the mesh was generated in the next code (PRATMESH) that the user could determine whether adequate resolution was attained. This is particularly true for regions of high gradients, such as the nacelle highlight. PRATPRE generates a file that contains the finite element nodal locations on the upper and lower surfaces of the nacelle, centerbody, and elements along the centerline of the nacelle upstream of the intersection of the centerbody and the duct centerline. Guidelines for the proper density of grid points relative to the frequency of the noise is given in Topol.[4] It is at this stage of the noise prediction that the user has the greatest input.

The output file for these data is fort.7 on the Silicon Graphics™ workstations. This file designation conflicts with the default error output file on the Hewlett Packard™ workstations (for the HP FORTRAN compiler, the FORTRAN created files are given the name of ftn. The fort.7 file on the Silicon Graphics workstation would, therefore, become ftn7 on the HP.) so the code had to be modified to write the finite element node locations to a separate file.

To create the input file for the PRATMESH mesh generation program, data specifying the relative placement of the finite element nodes on the fan face are added to the file containing the element node locations generated by the PRATPRE program. It was found that too many nodes on the fan face will cause the noise radiation component to crash without giving any errors. No output is written but the program appears to exit normally. The locations of the boundary of Region 2 of the mesh and the wave envelope boundaries are also specified in the PRATMESH input. Finally the circumferential mode

number, the number of radial modes that are to be solved, and the Mach number in the external flowfield are added to this file.

There are three components of the finite element mesh generated by PRATMESH: Region 1 which is largely interior to the nacelle, Region 2 which surrounds the nacelle in a relatively small band and the wave envelope region beyond Region 2 which forms a non-reflecting boundary to the computational domain. There are two reflecting boundaries on the domain, one along the centerline axis of symmetry and a 'baffle' downstream of the nacelle. Details on the different sections of the mesh and how to specify their dimensions can be found in Roy *et al.*[7] Also presented in this reference is a discussion on the degree to which the reflecting boundaries affect the acoustic solution.

There are several output files generated by PRATMESH. The file ftn20 contains details on the node location and the connectivity array and is required by all subsequent programs. It was found to be useful to save these files for future use rather than rerunning PRATMESH every time the duct Mach number was changed, for example. A *postscript* output file showing the mesh geometry (ftn14) is also generated by PRATMESH. An on-screen postscript viewing utility such as *Ghostview* was found to save a great deal time (and paper) when iterating on node location points. If the user wishes to save these plots as a postscript file, they should be renamed at this point since the subsequent components of the ARC each generate postscript files with the same name.

Flow Calculation

The potential flow problem is divided into three parts: the first is the free field (the flow is assumed to be aligned with the duct axis), the second is the flow around the nacelle, and the last is the flow due to the flow through the fan. The program PRATFLOW solves for the flow potential of the second and third of these three components individually. The program PRATVEL superposes the three components to give the velocity potential at the nodes and also computes the mean flow velocity. Both PRATFLOW and PRATVEL require the ftn20 file generated by PRATMESH. The potential flow problem is cast in incompressible form. That is instead of solving for the true compressible flow, the incompressible flowfield is solved and a compressibility correction applied to the solution.

Little input other than the type of solution desired is needed by PRATFLOW (it is possible to compute the flowfield due to the fan flow or the nacelle alone, rather than both). The input to PRATVEL is the free field flow conditions and the Mach number at the fan face.

PRATFLOW generates the program ftn21 and PRATVEL generates the program ftn22 both of which are required by the acoustic radiation component PRATRAD.

Acoustic Field Calculation

The final program used in the computation of the radiated noise field is PRATRAD. The input to this code includes the normalized frequency and the real and imaginary magnitudes of the duct acoustic modes. The normalized frequency, η, is defined thus

$$\eta = \frac{\omega R}{c} \tag{A1}$$

where ω is the rotational frequency of the fan in radians per second, R is the fan radius, and c is the speed of sound in the free stream. In addition to the input data file, the files ftn20, ftn21, and ftn22 (generated by PRATMESH, PRATFLOW and PRATVEL, respectively) must also be available.

Care must be exercised to ensure that the radial mode properties input to this code correspond to the angular mode specified in the PRATMESH program, i.e. the correct copies of the files ftn20, ftn21, and ftn22 are available. A possible improvement in future versions of this code may be to move the calculation of the duct mode properties that are now part of the mesh generation scheme to the PRATRAD stage of the computation. This would remove one of the parameters that now must be input into PRATRAD.

A further consideration is that the input to the radiation code is the amplitude of the real and imaginary parts of the modal pressure at the axial location where the data is known. In the ADP experiments described in section 6, a rotating microphone array was used to measure the acoustic modal amplitudes and phases in the nacelle. Although generically referred to as the fan face in the mesh generation stage, the better description would be the duct location where the modal information is known. In the case of a fan noise prediction code, such as V072 for example, the noise is calculated at the exit guide vane location.

There are two inputs to this program that require further clarification. The first is that the input to this code also includes an instruction as to whether the computation is for a rectangular or axisymmetric duct. In this version of the program, however, the rectangular duct solution is not operable. Second, there is provision for acoustic liner data to be specified. Improvements to this liner model are to be made in later versions of this program.

The output files of the radiation code as supplied does not contain all the nodal information on the real and imaginary pressure components of the acoustic field. To retrieve this data, the code must be modified in the following way. In the subroutine "GEPOST" there is a section of code commented out that refers to the plotting routine "TECPLOT." An output file can be opened at this point to which the data arrays containing the nodal coordinates, the real and imaginary components of the acoustic pressure and the velocity at the nodes can be written. These data can then be plotted with the users graphics program.

The PRATRAD code generates a postscript file (as with the other components, under the name ftn14) containing a polar contour plot of the acoustic potential, a plot of the SPL directivity and the pressure directivity and polar contour plots of the SPL directivity and acoustic pressure. The SPL data in these figures have been normalized so that the highest level is 100 dB. This was done to provide relative SPL for the case of the artificial input data. If the user has actual input pressure levels and wishes to see true predictions of the sound pressure level, the code must be modified in the subroutine GEPOST to remove this normalization (the normalization takes place in the same vicinity as the TECPLOT reference). In the course of investigating different geometries than the test case supplied with the code it was found that these plotting routines would sometimes crash. This is currently attributed to the geometry and input parameters of the test subject but is still under investigation.

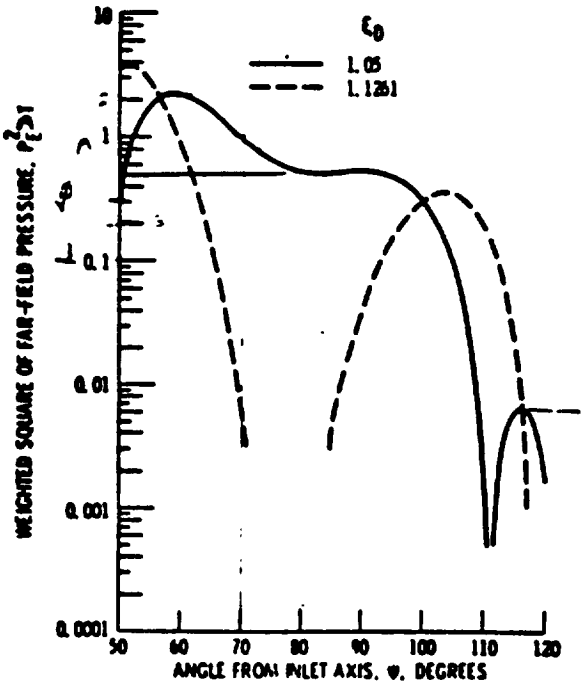

(a)

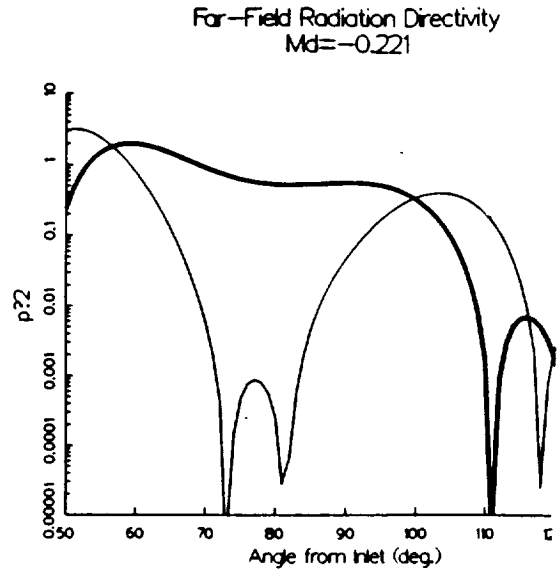

(b)

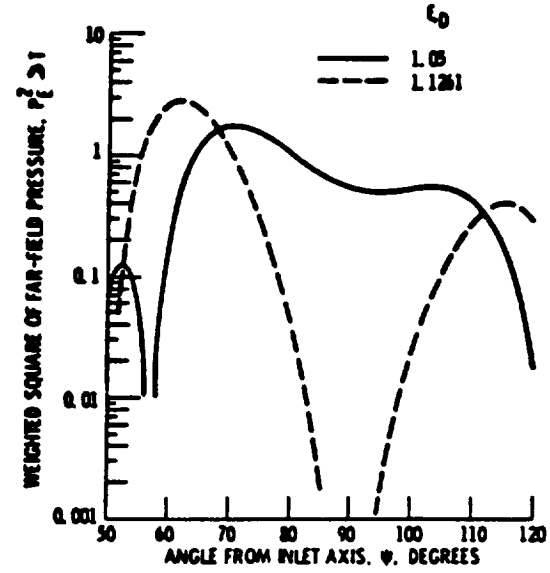

(c)

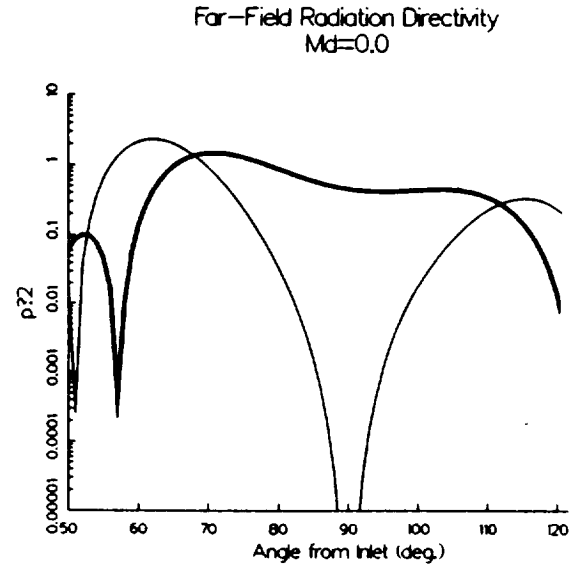

(d)

Figure 1 Test Cases demonstrating correct implementation of the cutoff ratio technique. Figures (a) and (c) from reference 3, figures (b) and (d) from current implementation.

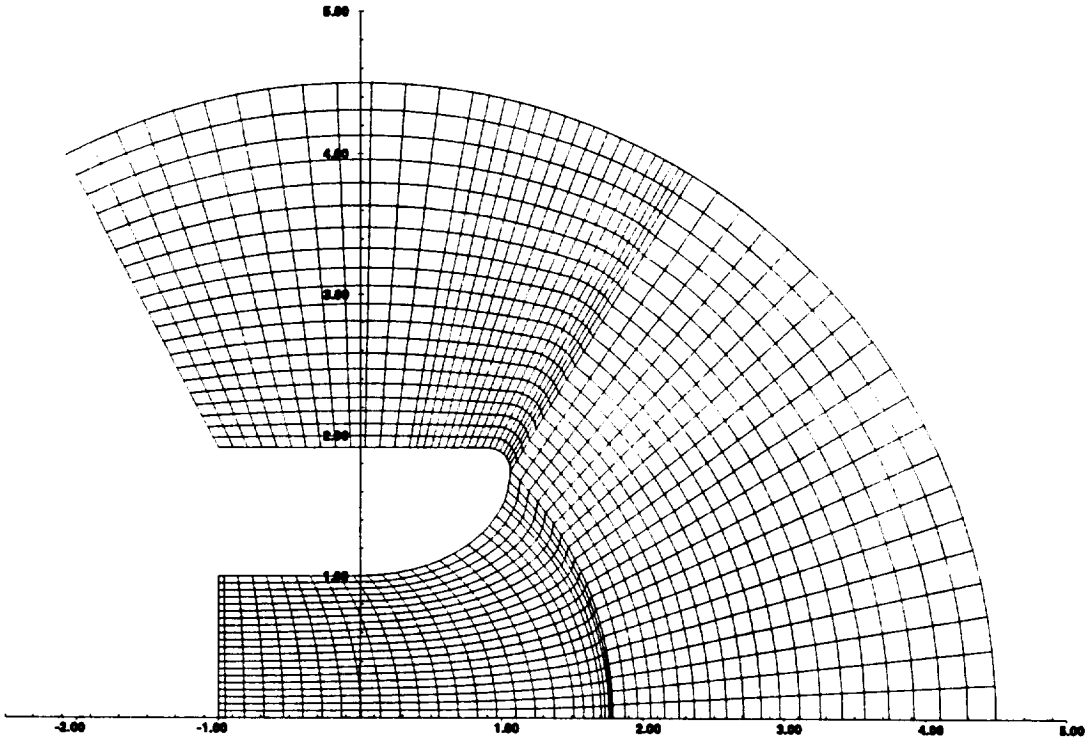

Figure 2 Bellmouth geometry. Partial grid used in the ARC calculation is shown.

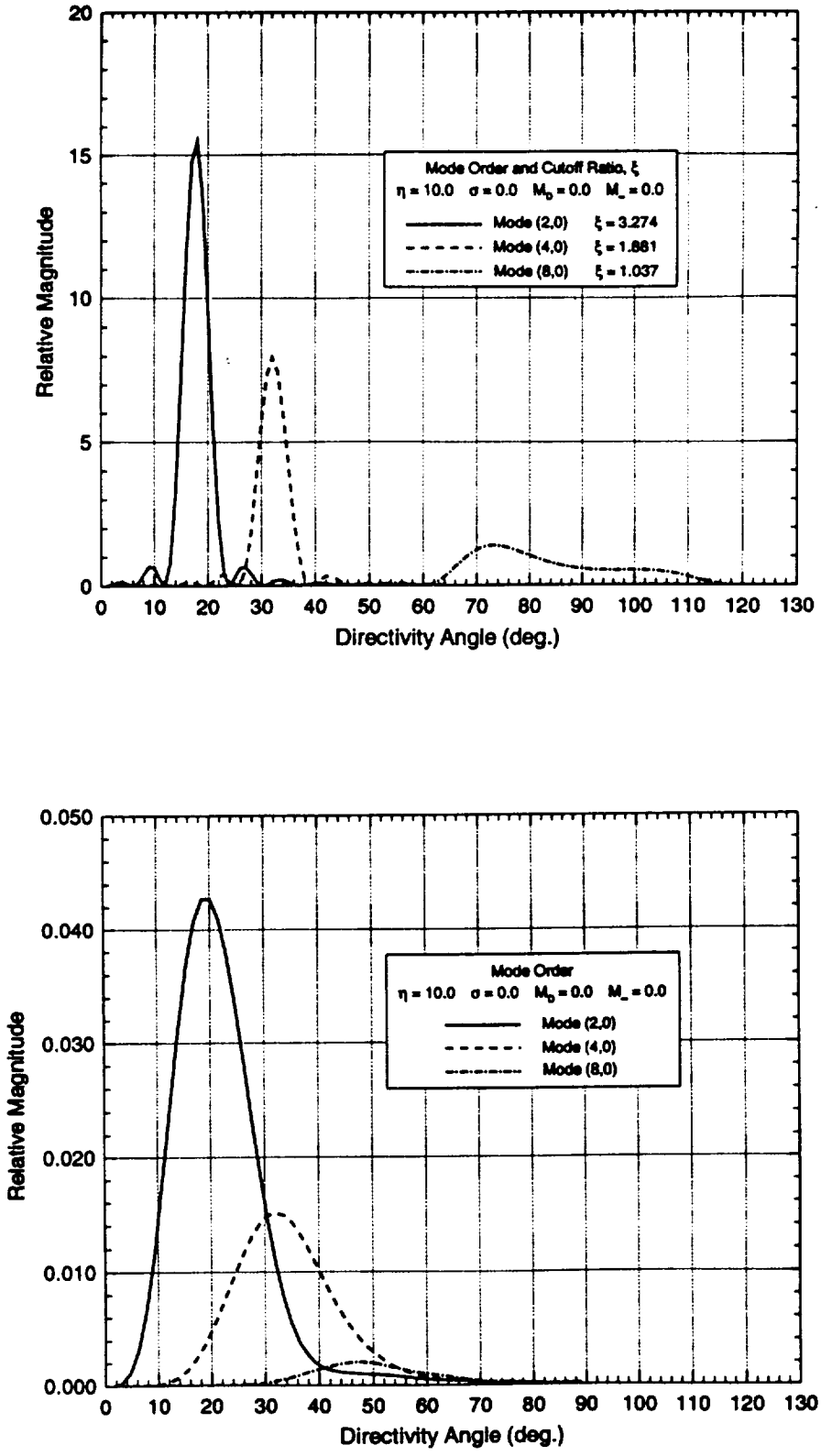

Figure 3 Influence of circumferential mode order on farfield noise directivity. Upper figure generated with cutoff ratio technique, lower figure generated with ARC.

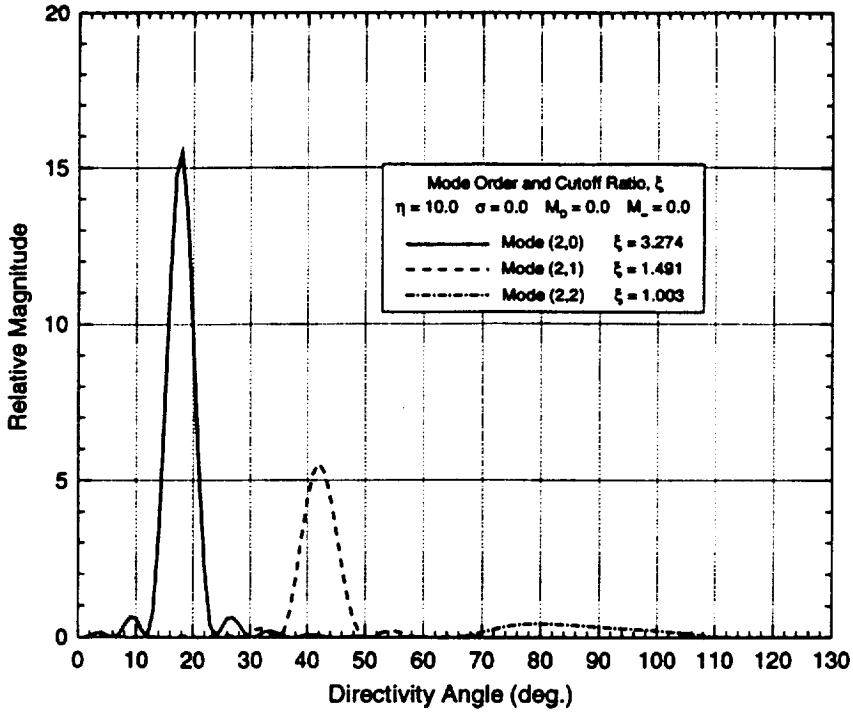

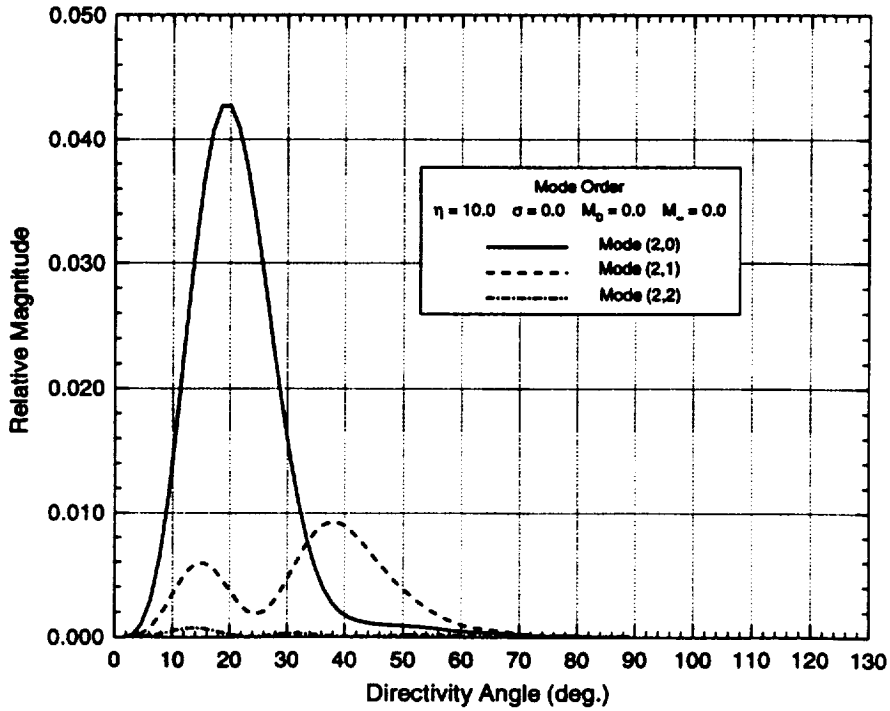

Figure 4 Influence of radial mode order on farfield noise directivity. Upper figure generated with cutoff ratio technique, lower figure generated with ARC.

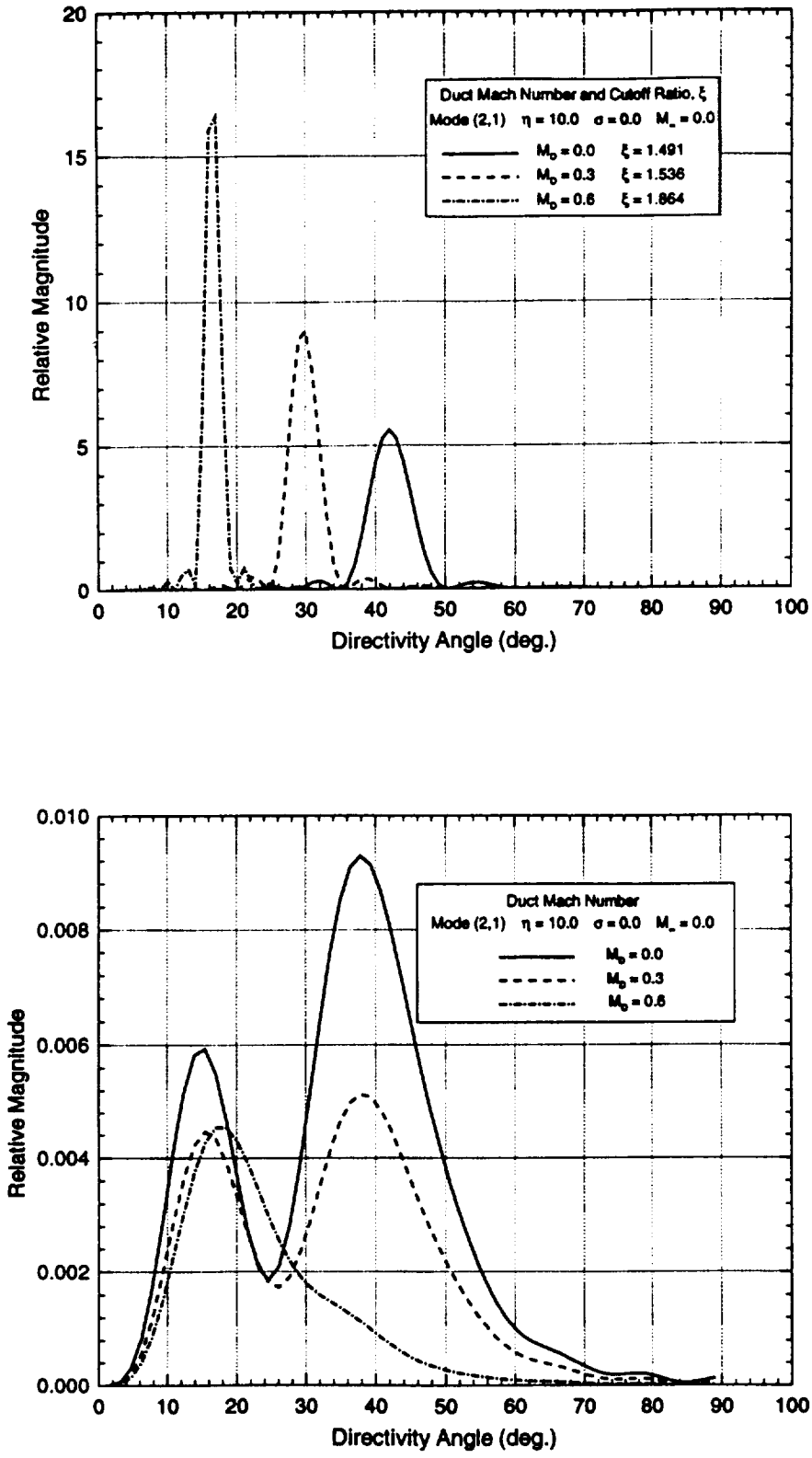

Figure 5 Influence of duct Mach number on farfield noise directivity. Upper figure generated with cutoff ratio technique, lower figure generated with ARC.

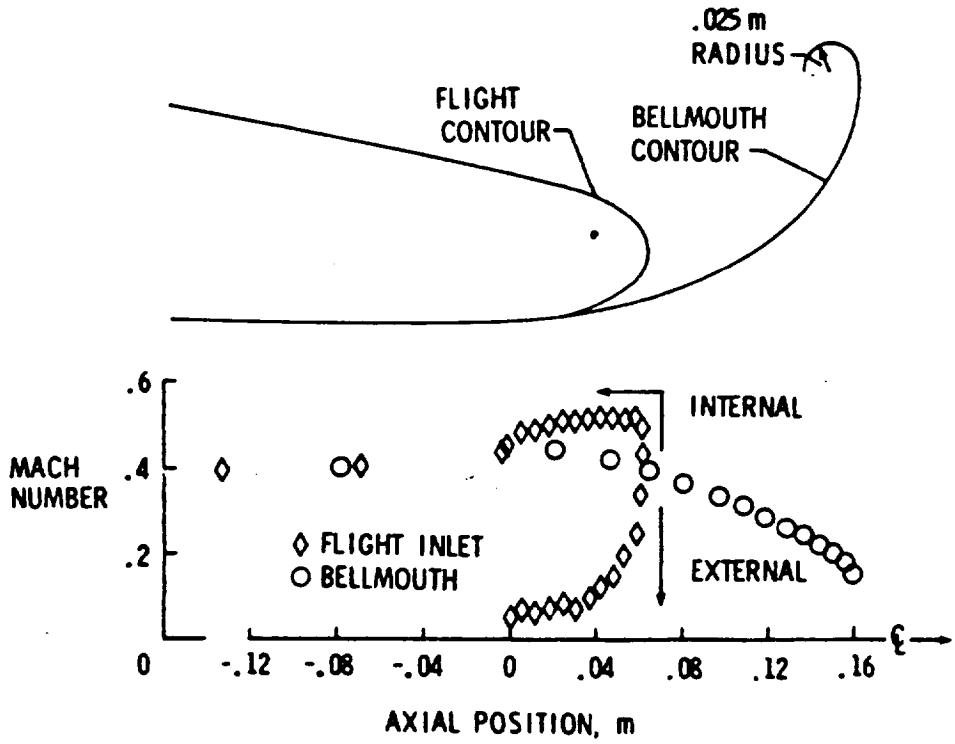

Figure 6 Schematic diagram of the flight and bellmouth inlets from reference 5. Also shown is the measured inlet Mach number distribution for each configuration for the case of $M_D = 0.4$.

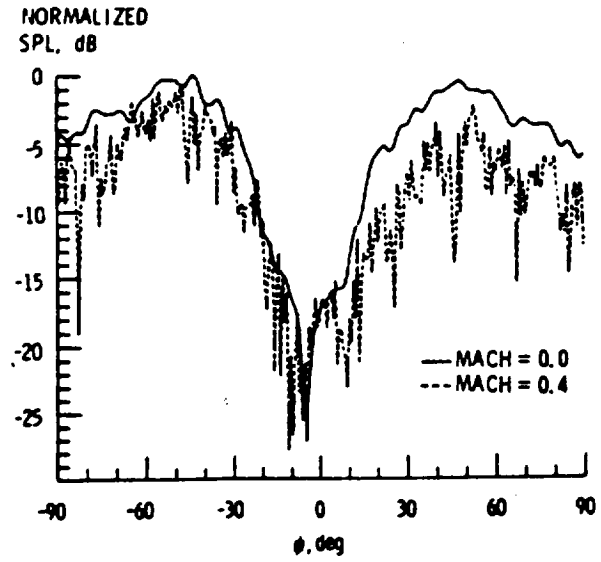

Figure 7 Measured directivity of the 'flight' inlet for mode (2,0), $\eta = 3.72$

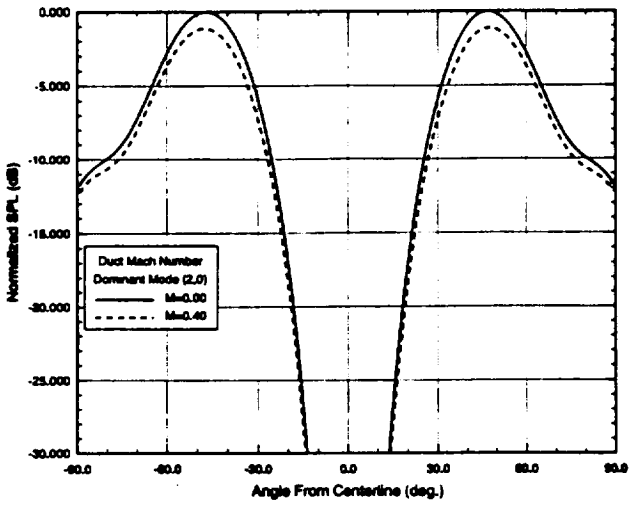

Figure 8 ARC computed directivity of the 'flight' inlet for mode (2,0), $\eta = 3.72$.

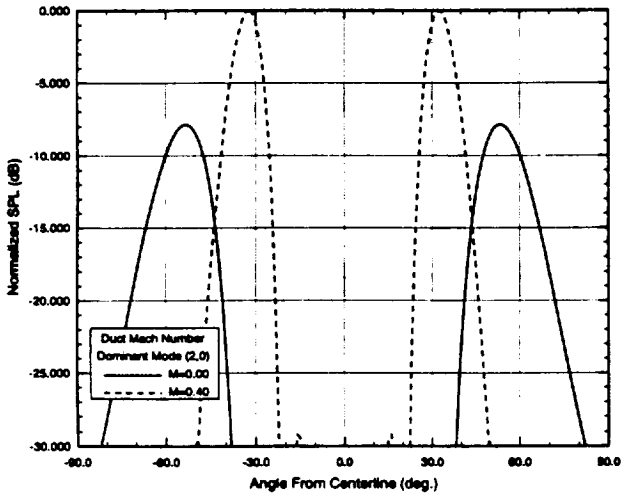

Figure 9 Cutoff ratio computed directivity of the 'flight' inlet for mode (2,0), $\eta = 3.72$

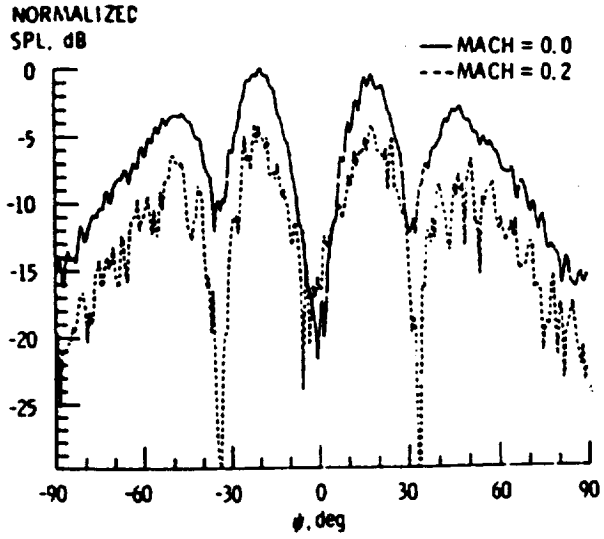

Figure 10 Measured directivity of the bellmouth inlet for modes (2,0) and (2,1), η = 8.18.

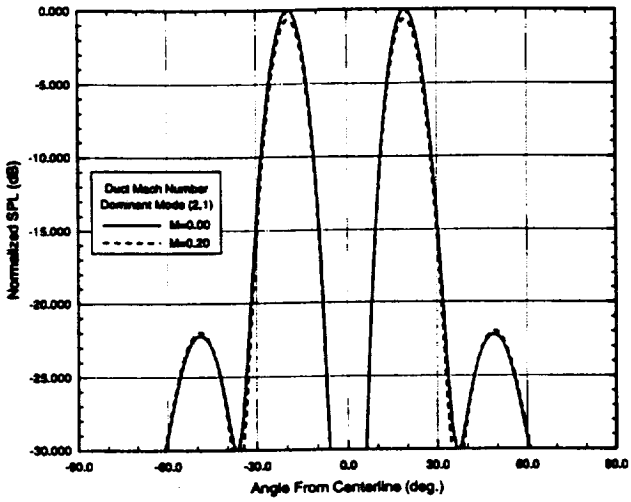

Figure 11 ARC computed directivity of the bellmouth inlet for modes (2,0) and (2,1), η = 8.18.

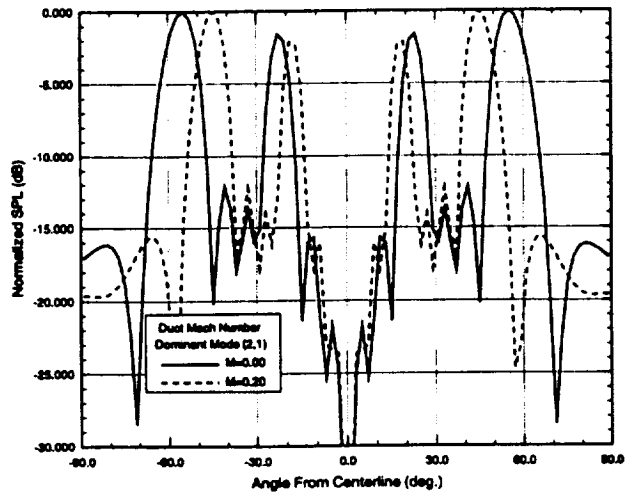

Figure 12 Cutoff ratio computed directivity of the bellmouth inlet for modes (2,0) and (2,1), η = 8.18.

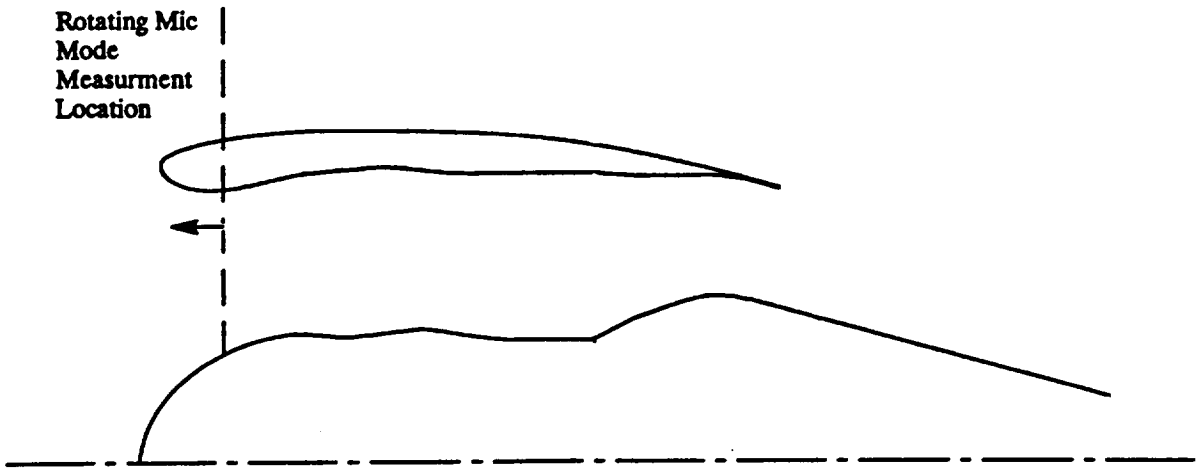

b) Medium Inlet Nacelle, Short Spinner

Figure 13 Schematic diagram of the 17 inch diameter ADP model from reference 4.

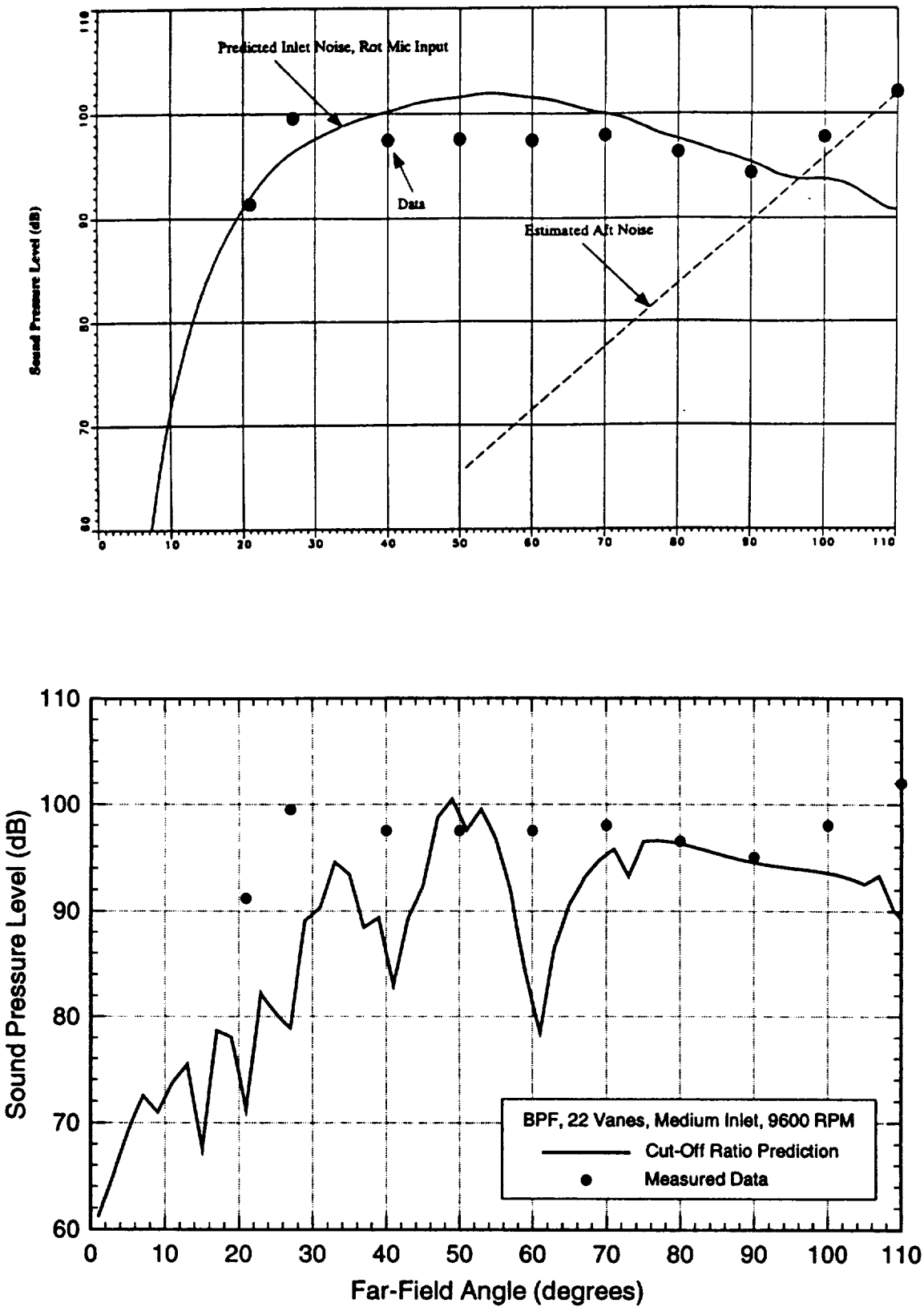

Figure 14 Farfield noise predictions for the ADP at Blade Passage Frequency (BPF). Medium inlet, 22 exit guide vanes, 9600 RPM. Upper figure: ARC prediction, lower figure: cutoff ratio prediction.

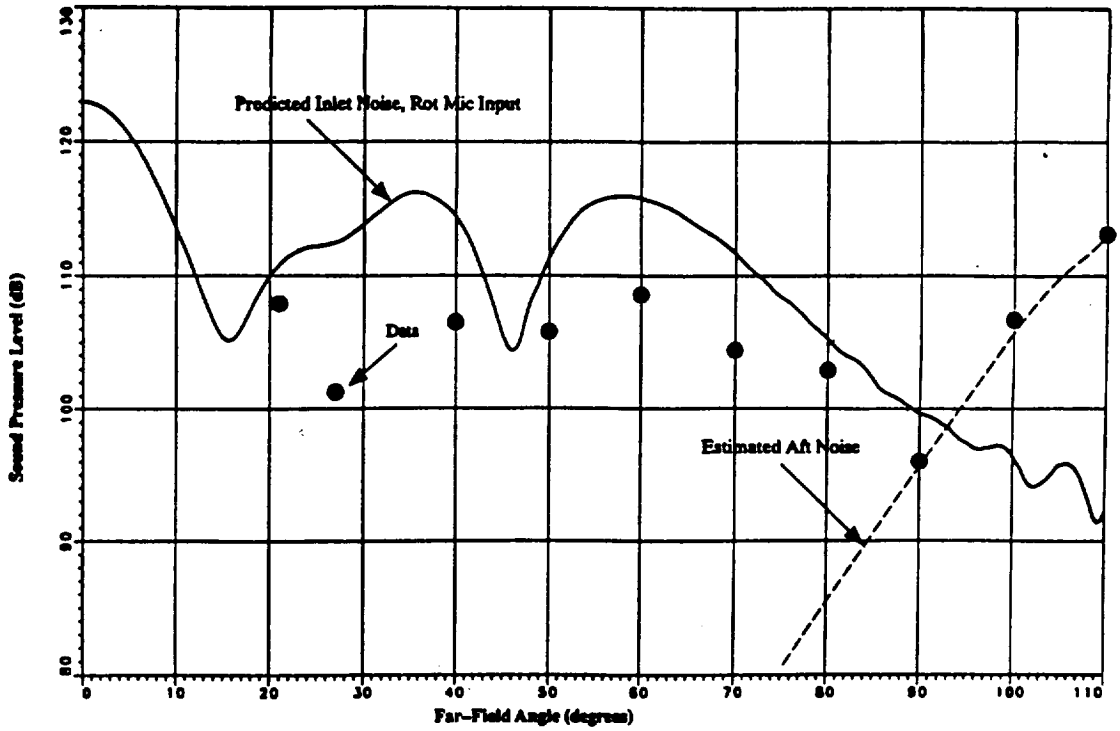

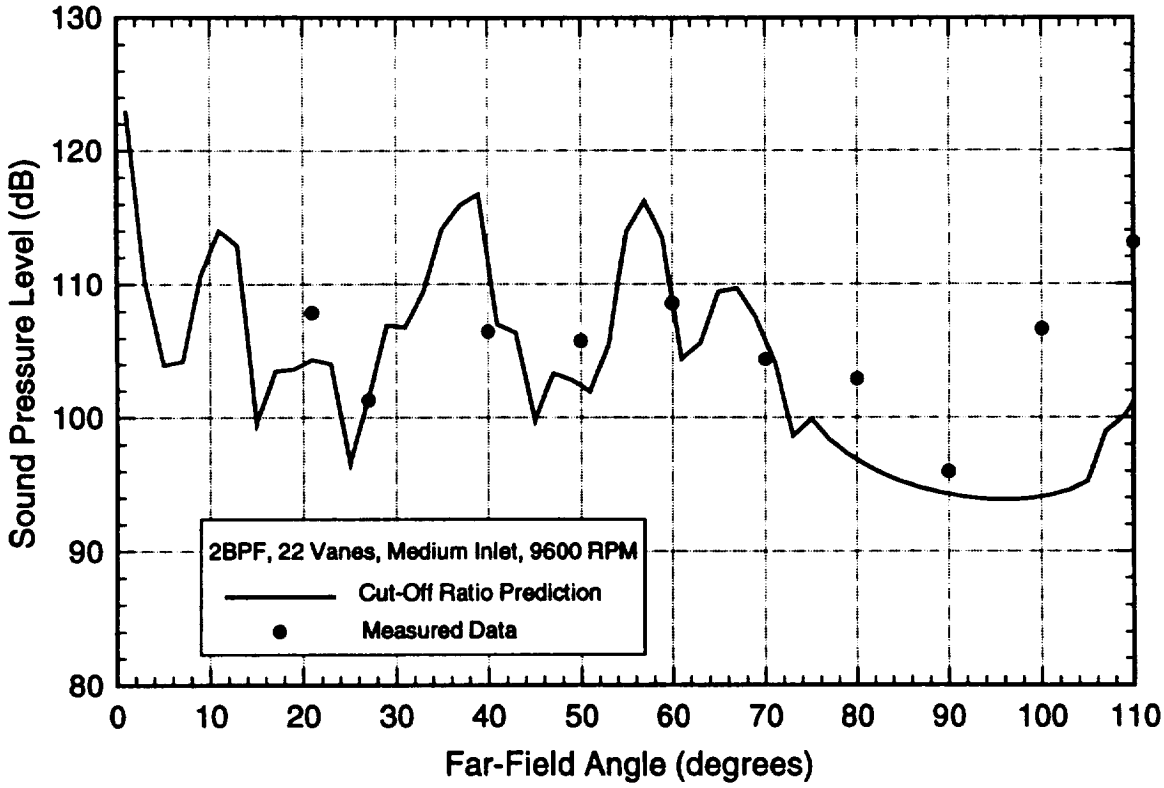

Figure 15 Farfield noise predictions for the ADP at twice Blade Passage Frequency (2BPF). Medium inlet, 22 exit guide vanes, 9600 RPM. Upper figure: ARC prediction, lower figure: cutoff ratio prediction.

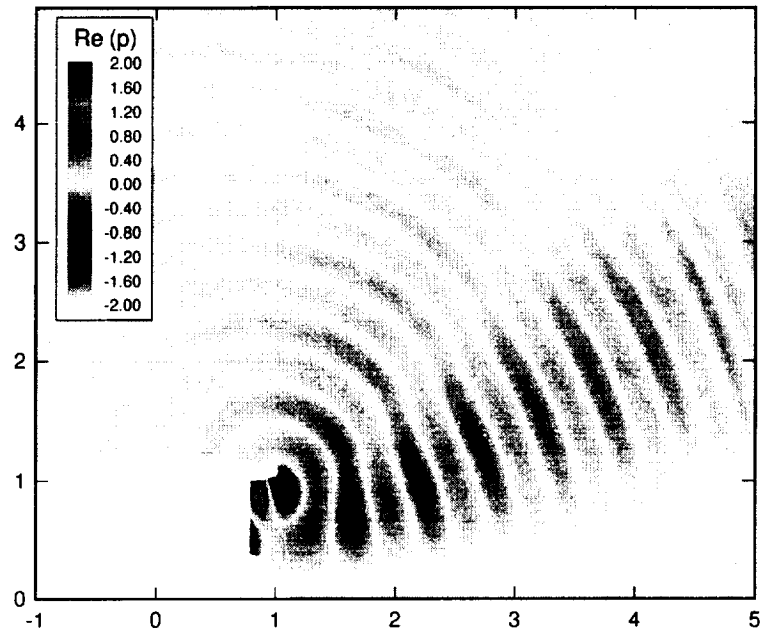

Figure 16 Noise pressure contour plot for modes (4,0) and (4,1) with original phase.

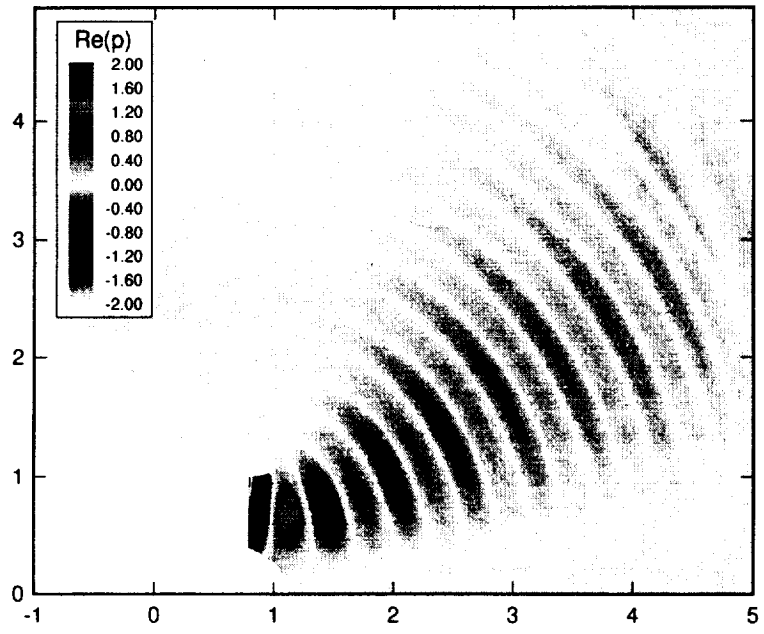

Figure 17 Noise pressure contour plot for modes (4,0) and (4,1) with modified phase.

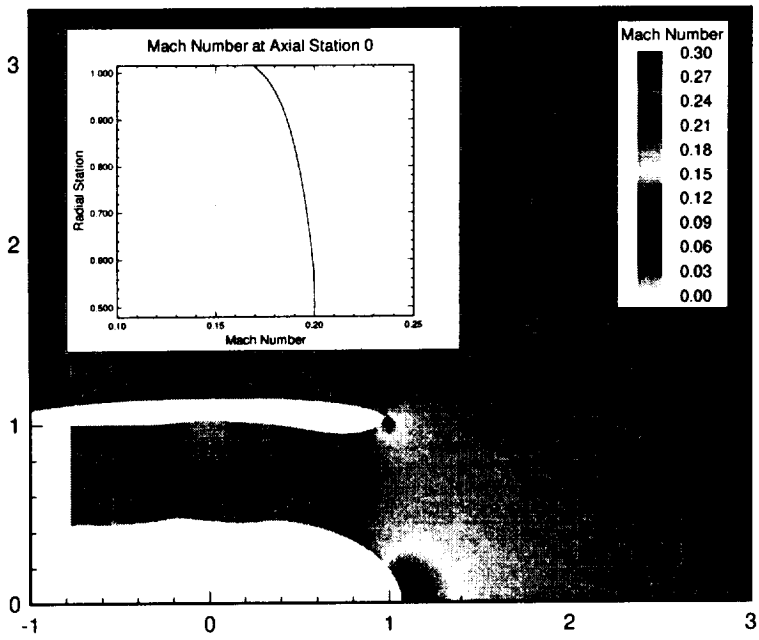

Figure 18 ARC prediction of the Mach number distribution for M_D =0.2 and M_∞ =0.2

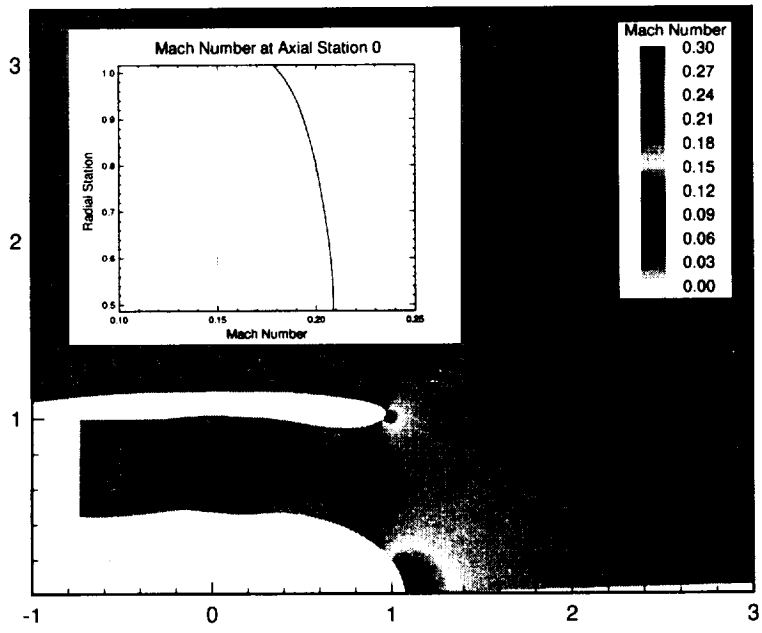

Figure 19 CPFS prediction of the Mach number distribution for M_D =0.2 and M_∞ =0.2

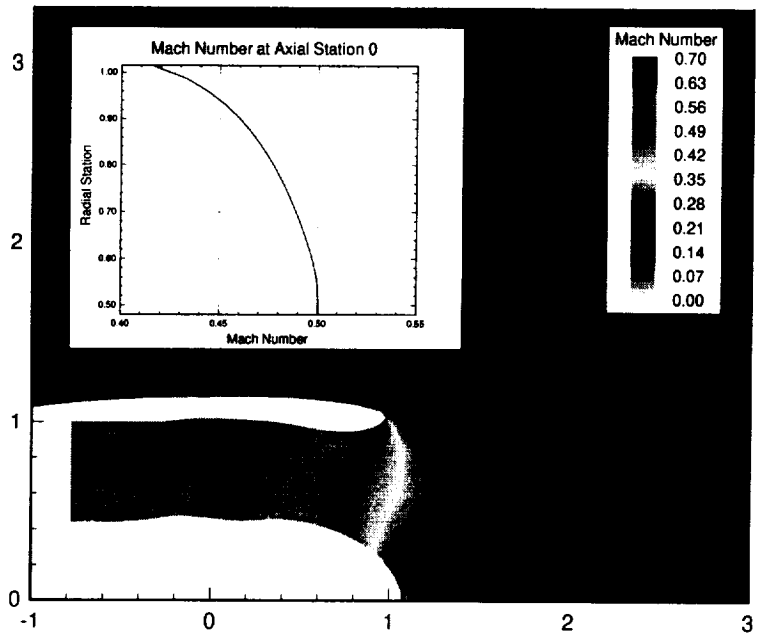

Figure 20 ARC prediction of the Mach number distribution for M_D =0.5 and M_∞ =0.2

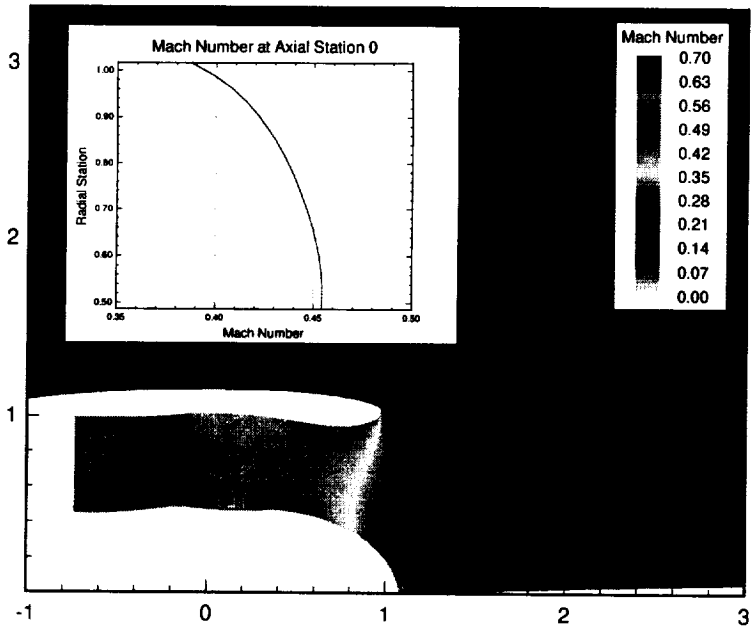

Figure 21 CPFS prediction of the Mach number distribution for M_D =0.5 and M_∞ =0.2

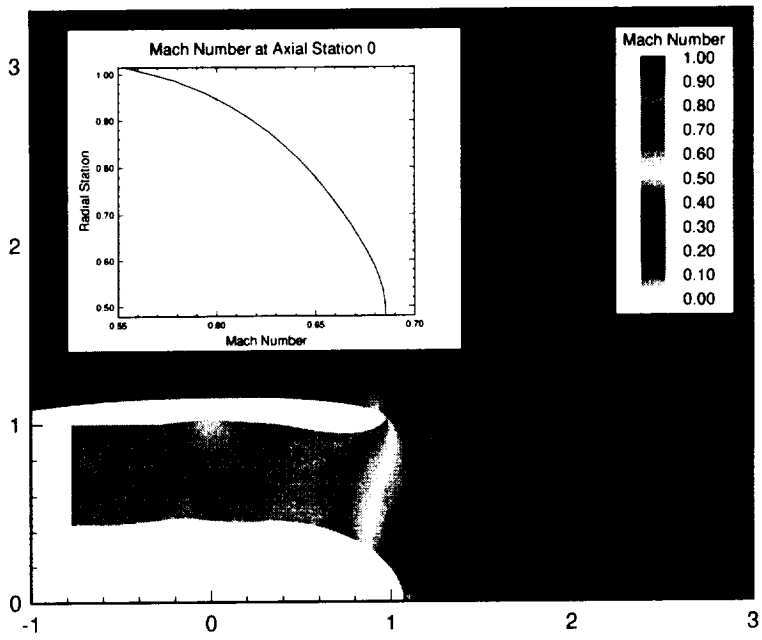

Figure 22 ARC prediction of the Mach number distribution for M_D =0.7 and M_∞ =0.2

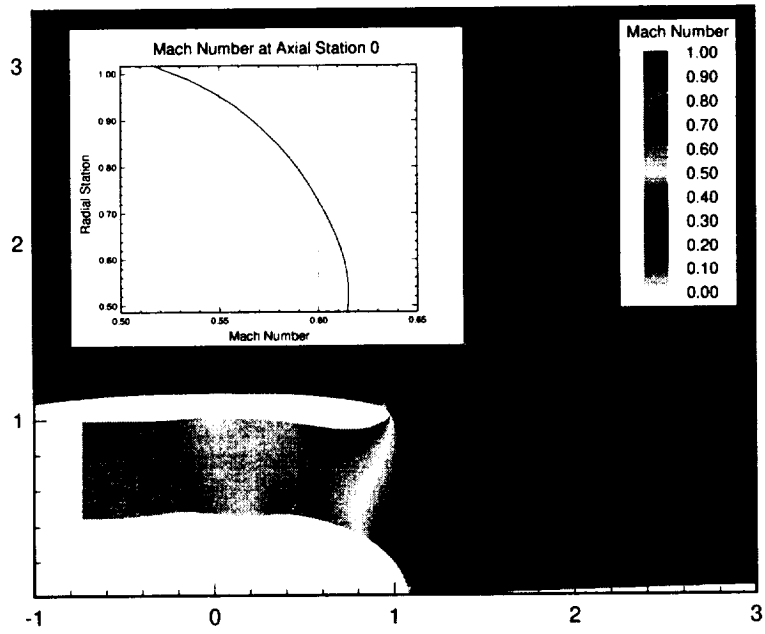

Figure 23 CPFS prediction of the Mach number distribution for M_D =0.7 and M_∞ =0.2

REPORT DOCUMENTATION PAGE

Form Approved
OMB No. 0704-0188

1. AGENCY USE ONLY (*Leave blank*)	2. REPORT DATE	3. REPORT TYPE AND DATES COVERED
	May 1995	Contractor Report

4. TITLE AND SUBTITLE
Fan Noise Prediction Assessment

5. FUNDING NUMBERS
NAS1-20103, Task 3
538-03-11-01

6. AUTHOR(S)
Paul H. Bent

7. PERFORMING ORGANIZATION NAME(S) AND ADDRESS(ES)
McDonnell Douglas Aerospace
Acoustic Technology, Mail Code 71-35
1510 Hughes Way
Long Beach, CA 90810-1864

8. PERFORMING ORGANIZATION REPORT NUMBER
CRAD-9310-TR-0128

9. SPONSORING / MONITORING AGENCY NAME(S) AND ADDRESS(ES)
National Aeronautics and Space Administration
Langley Research Center
Hampton, VA 23681-0001

10. SPONSORING / MONITORING AGENCY REPORT NUMBER
NASA CR-195051

11. SUPPLEMENTARY NOTES
Langley Technical Monitor: Joe W. Posey
Final Report

12a. DISTRIBUTION / AVAILABILITY STATEMENT
Unclassified - Unlimited

Subject Category 71

12b. DISTRIBUTION CODE

13. ABSTRACT (*Maximum 200 words*)

This report is an evaluation of two techniques for predicting the fan noise radiation from engine nacelles. The first is a relatively computational intensive finite element technique. The code is named ARC, an abbreviation of Acoustic Radition Code, and was developed by Eversman. This is actually a suite of software that first generates a grid around the nacelle, then solves for the potential flowfield, and finally solves the acoustic radiation problem.

The second approach is an analytical technique requiring minimal computational effort. This is termed the cutoff ratio technique and was developed by Rice. Details of the duct geometry, such as the hub-to-tip ratio and Mach number of the flow in the duct, and modal content of the duct noise are required for proper prediction.

14. SUBJECT TERMS
Fan Noise Prediction, Duct Noise Radiation, Fan Noise Radiation, Duct Modes

15. NUMBER OF PAGES
36

16. PRICE CODE
A03

17. SECURITY CLASSIFICATION OF REPORT	18. SECURITY CLASSIFICATION OF THIS PAGE	19. SECURITY CLASSIFICATION OF ABSTRACT	20. LIMITATION OF ABSTRACT
Unclassifed	Unclassified		